Manipulating Ru Oxidation within Electrospun Carbon Nanofibers to Boost Hydrogen and Oxygen Evolution for Electrochemical Overall Water Splitting

Mengxiao Zhong, Su Yan, Jiaqi Xu, Ce Wang, Xiaofeng Lu*

Alan G. MacDiarmid Institute, College of Chemistry, Jilin University, 2699 Qianjin Street, Changchun 130012, P. R. China.

*Corresponding author.

Email address: xflu@jlu.edu.cn (Prof. X. Lu)

Measurements of the calibration of Hg/HgO electrode

The Hg/HgO electrode as the reference electrode was calibrated by a relatively steady state chronoamperometry method in H_2-saturated 1 M KOH. Two polished Pt foils with the same area served as working electrode and counter electrode to form a three-electrode system. A series of chronoamperometry curves were measured for 300 s to get the current interconvert between the hydrogen oxidation and hydrogen evolution reaction. The potential at zero net current was obtained from the figure plotting the currents at 300 s with the corresponding applied potentials. In this study, the potential of zero net current was found at -0.928 V vs. Hg/HgO (Fig. S1). Therefore, the potentials were transferred to reversible hydrogen electrode (RHE) via the Nernst equation: $E_{RHE} = E_{Hg/HgO} + 0.928$ V.

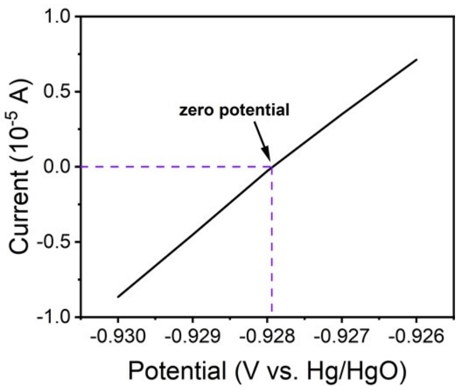

Fig. S1 The current as a function of the applied potentials for the calibration of Hg/HgO reference electrode.

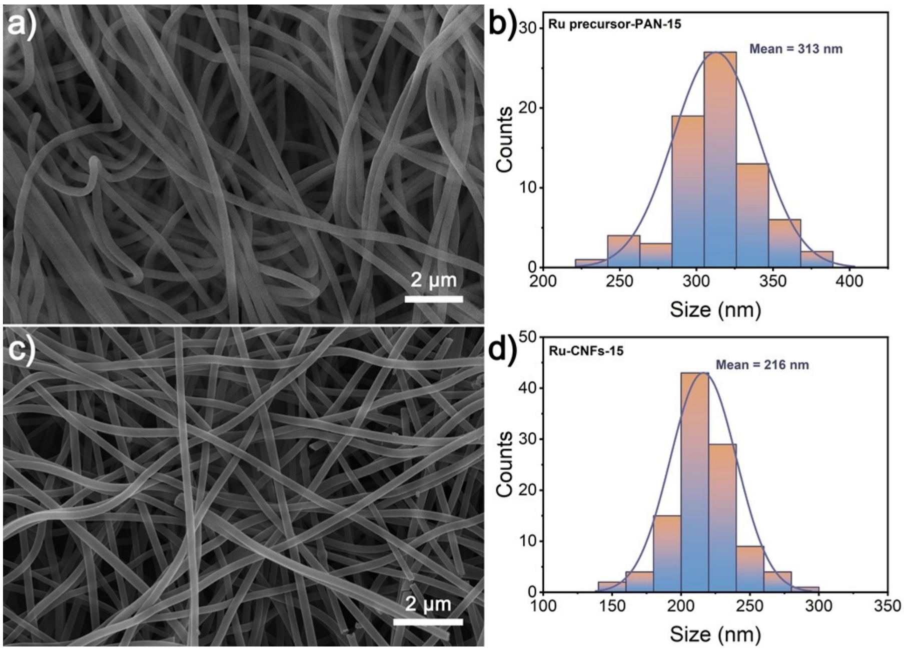

Fig. S2 SEM images of (a) Ru precursor-PAN-15 and (c) Ru-CNFs-15. Statistic histograms of the diameter distribution of (b) Ru precursor-PAN-15 and (d) Ru-CNFs-15.

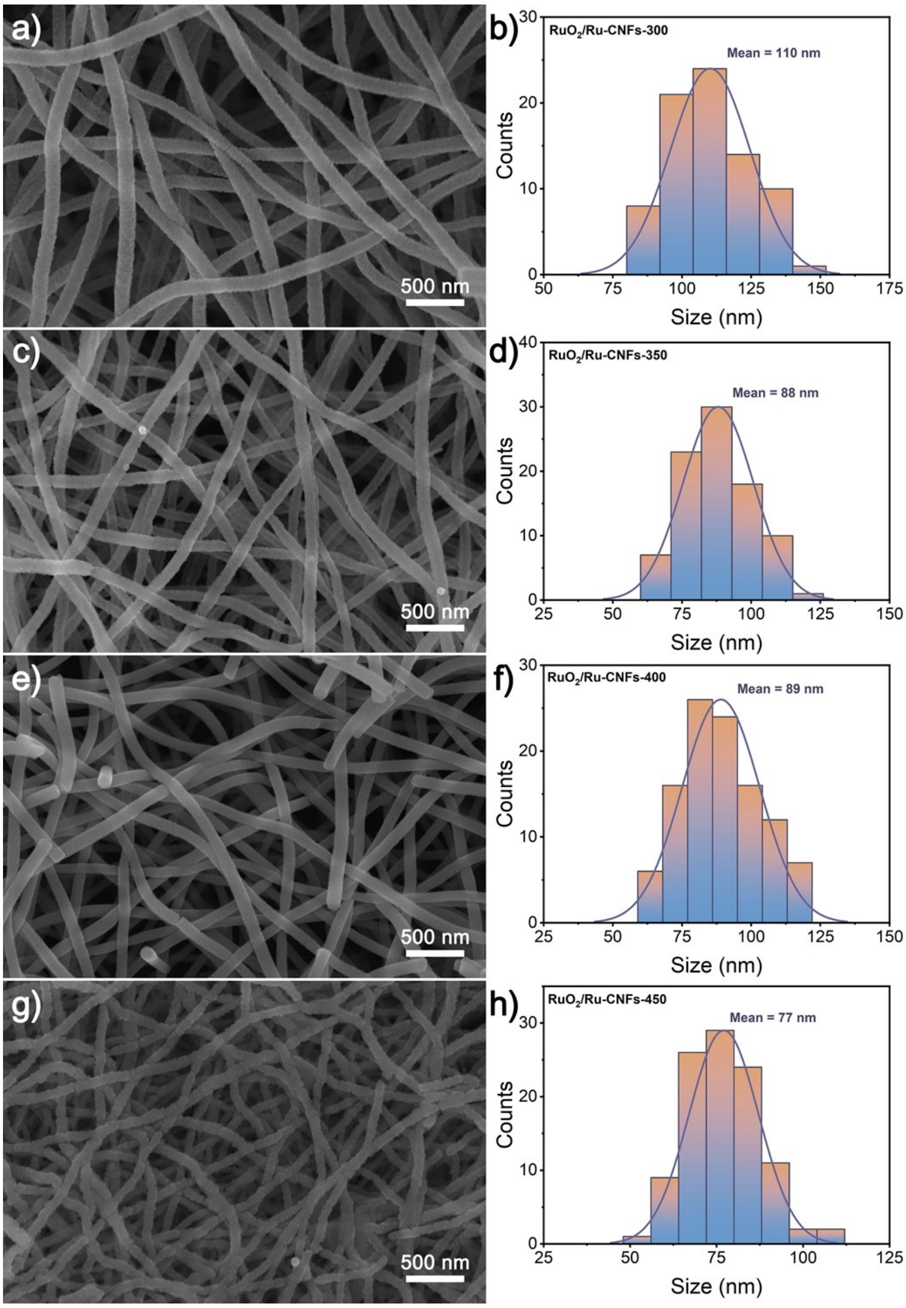

Fig. S3 SEM images of (a) RuO_2/Ru-CNFs-300, (c) RuO_2/Ru-CNFs-350, (e) RuO_2/Ru-CNFs-400 and (g) RuO_2/Ru-CNFs-450. Statistic histograms of the diameter distribution of (b) RuO_2/Ru-CNFs-300, (d) RuO_2/Ru-CNFs-350, (f) RuO_2/Ru-CNFs-400 and (h) RuO_2/Ru-CNFs-450.

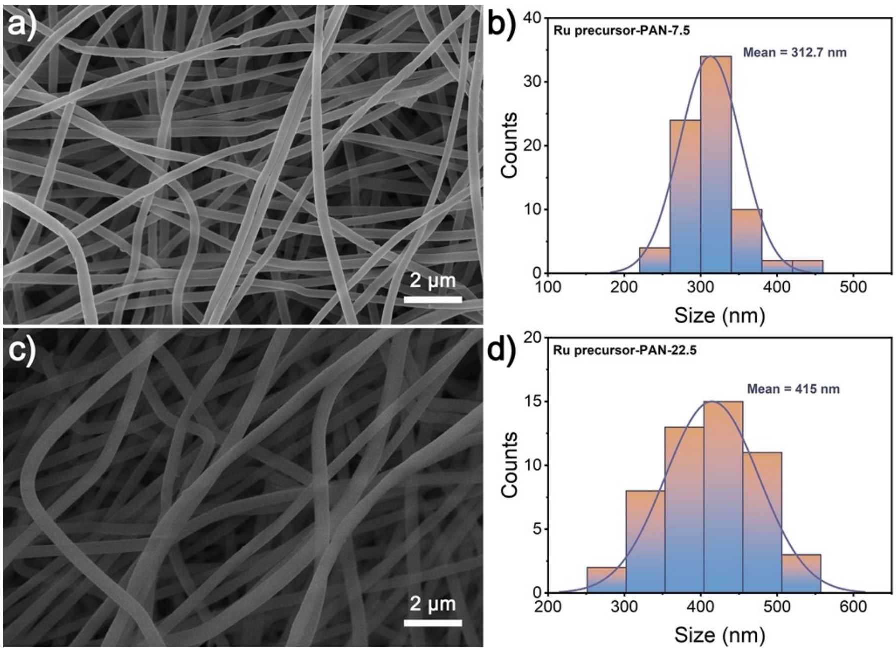

Fig. S4 SEM images of (a) Ru precursor-PAN-7.5 and (c) Ru precursor-PAN-22.5. Statistic histograms of the diameter distribution of (b) Ru precursor-PAN-7.5 and (d) Ru precursor-PAN-22.5.

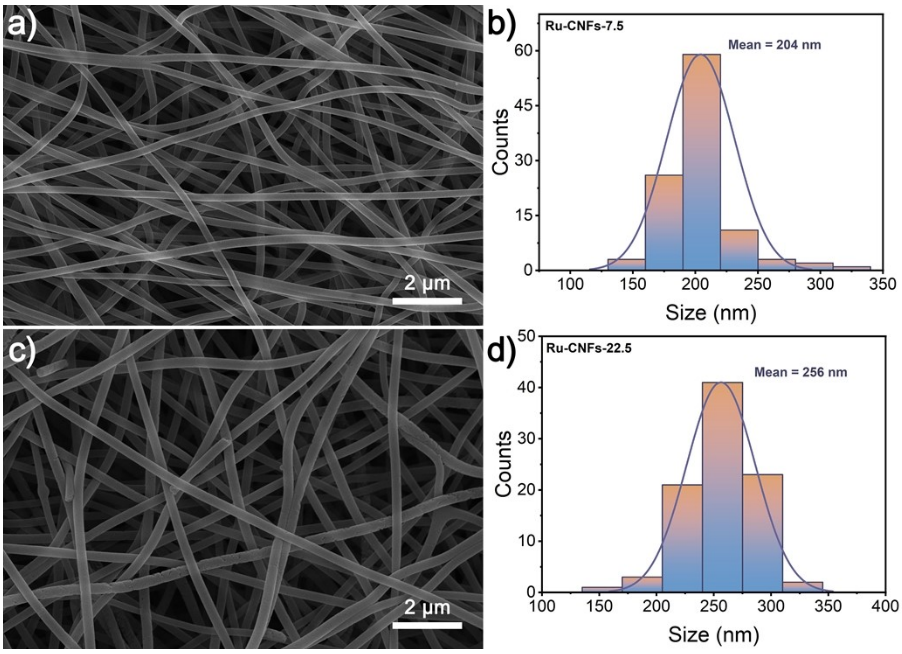

Fig. S5 SEM images of (a) Ru-CNFs-7.5 and (c) Ru-CNFs-22.5. Statistic histograms of the diameter distribution of (b) Ru-CNFs-7.5 and (d) Ru-CNFs-22.5.

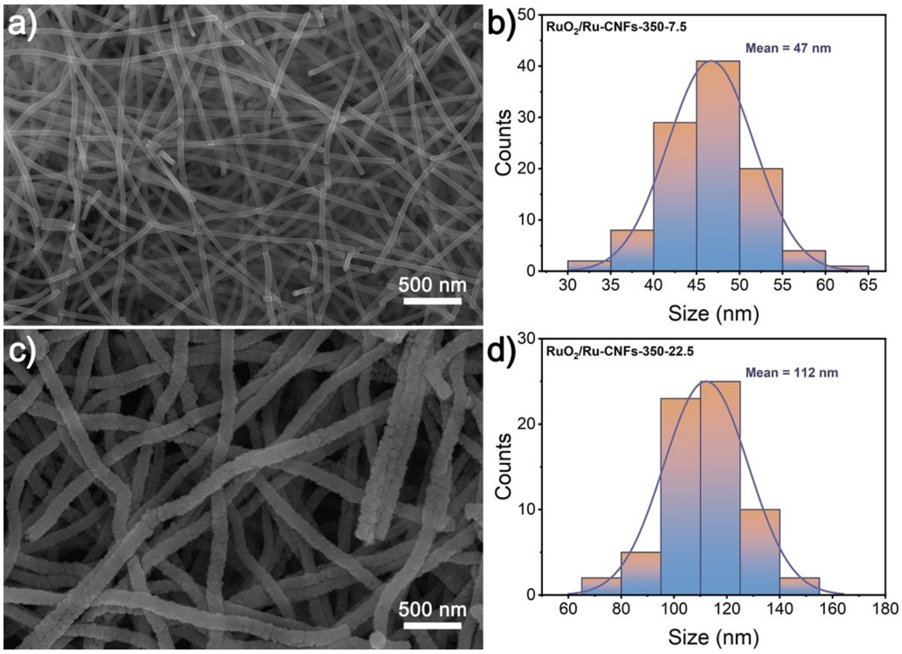

Fig. S6 SEM images of (a) RuO_2/Ru-CNFs-350-7.5 and (c) RuO_2/Ru-CNFs-350-22.5. Statistic histograms of the diameter distribution of (b) RuO_2/Ru-CNFs-350-7.5 and (d) RuO_2/Ru-CNFs-350-22.5.

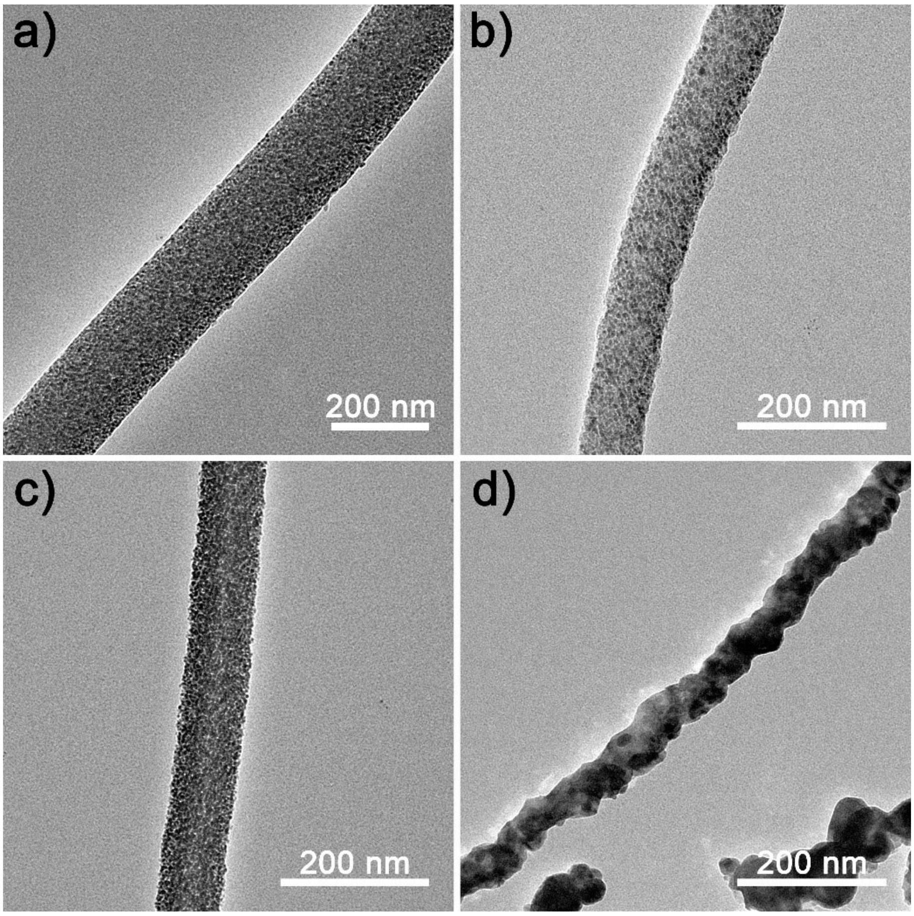

Fig. S7 TEM images of (a) Ru-CNFs-15, (b) RuO_2/Ru-CNFs-300, (c) RuO_2/Ru-CNFs-400 and (d) RuO_2/Ru-CNFs-450.

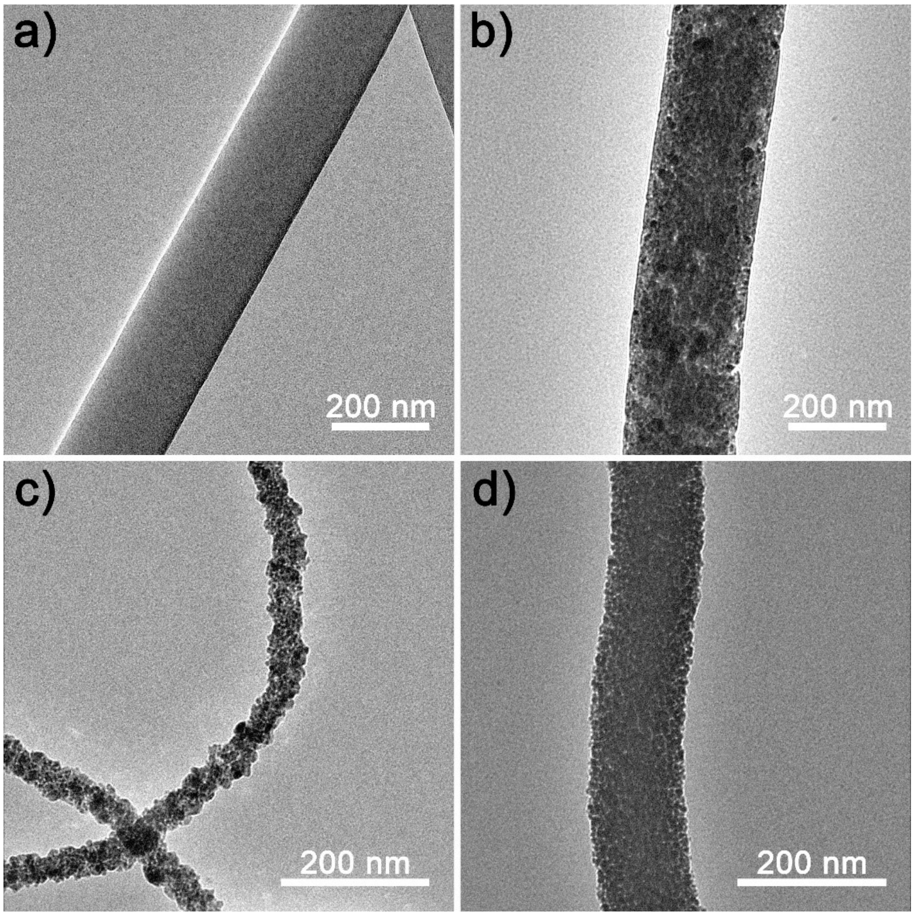

Fig. S8 TEM images of (a) Ru-CNFs-7.5 and (b) Ru-CNFs-22.5, (c) RuO_2/Ru-CNFs-350-7.5 and (d) RuO_2/Ru-CNFs-350-22.5.

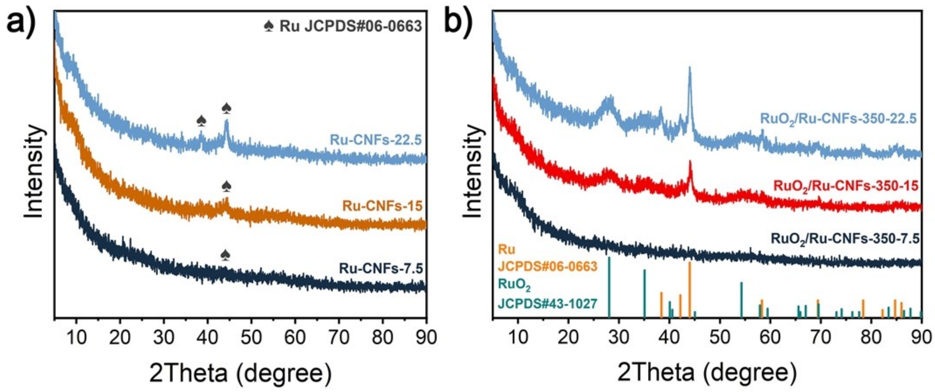

Fig. S9 (a) XRD patterns of Ru-CNFs-7.5, Ru-CNFs-15 and Ru-CNFs-22.5. (b) XRD patterns of RuO_2/Ru-CNFs-350-7.5, RuO_2/Ru-CNFs-350-15 and RuO_2/Ru-CNFs-350-22.5.

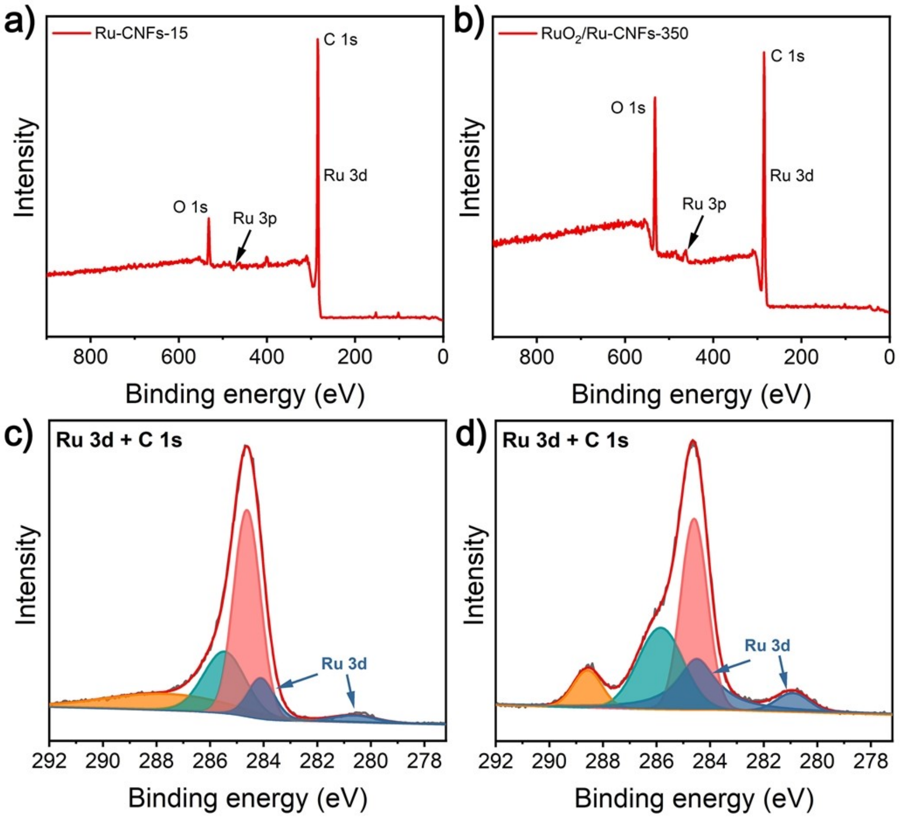

Fig. S10 (a) Full survey and (c) narrow-scan XPS spectrum of Ru-CNFs-15. (b) Full survey and (d) narrow-scan XPS spectrum of RuO_2/Ru-CNFs-350.

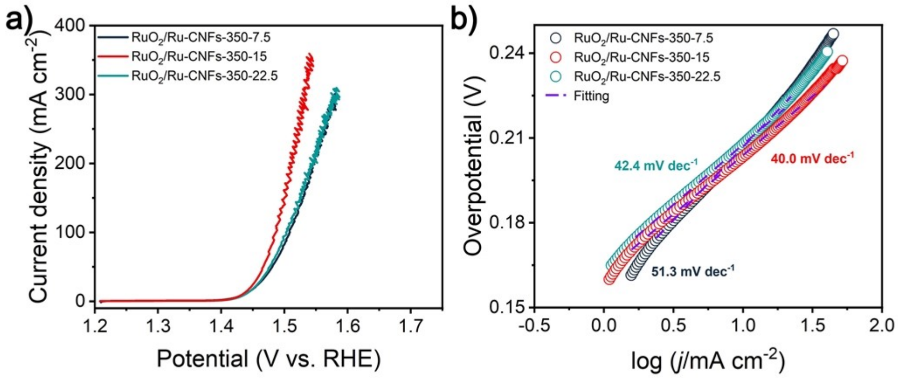

Fig. S11 (a) Polarization curves and (b) Tafel plots of different RuO_2/Ru-CNFs catalysts for OER in 1 M KOH.

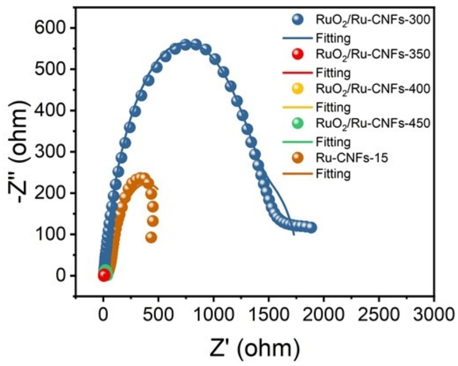

Fig. S12 Nyquist plots of different catalysts for OER. The dots and lines represent the experimental and fitting data, respectively.

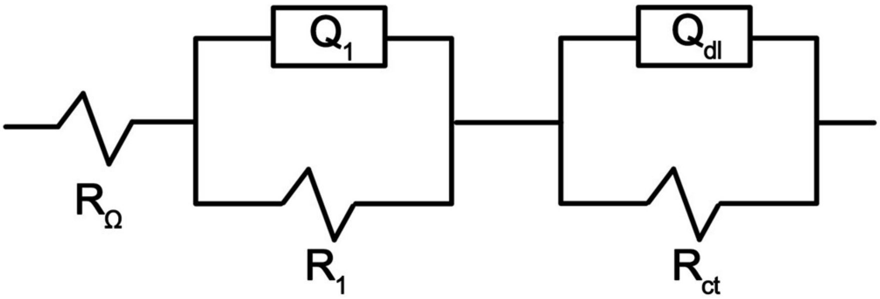

Fig. S13 The equivalent circuit model of electrodes. R_{Ω} is cell resistance including the connections, the electrolyte, and oxide deposit resistance; R_{ct} is the charge transfer resistance; R_1 is the contact resistance between the catalyst and electrode, Q_1 and Q_{dl} are the signs of the constant phase element and the double-layer capacitance, respectively.

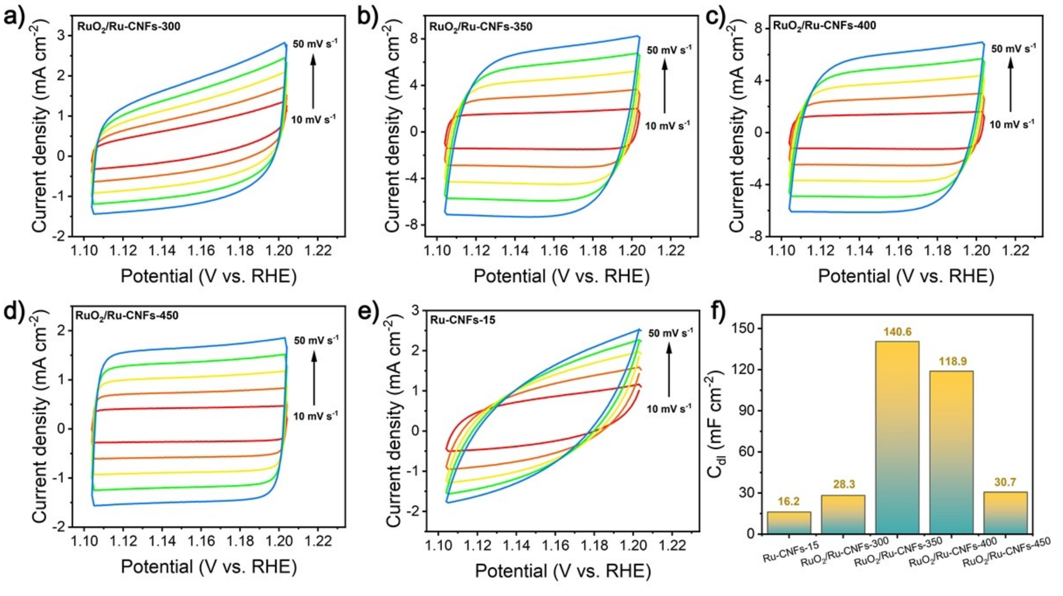

Fig. S14 CV curves with different scan rates from 10 to 50 mV s^{-1} in the region of 1.104-1.204 V *vs.* RHE for (a) RuO_2/Ru-CNFs-300, (b) RuO_2/Ru-CNFs-350, (c) RuO_2/Ru-CNFs-400, (d) RuO_2/Ru-CNFs-450 and (e) Ru-CNFs-15, respectively. (f) C_{dl} values of different catalysts.

Estimation of ECSA

The ECSA value was evaluated from the double layer capacitance (C_{dl}), which was determined by a CV method. The CV measurements were proceeded in a potential range of 1.104-1.204 V *vs.* RHE (with no Faradic responses) at different scan rates of 10, 20, 30, 40 and 50 mV s^{-1}. Then, C_{dl} values were calculated by plotting capacitive current density Δj (j_{anode}-$j_{cathode,}$ acquired from the corresponding CV curves) at 1.154 V *vs.* RHE versus scan rate, and the linear slope value is twice to the C_{dl}. Thus, the ECSA values can be estimated according to the following equation: ECSA = $(C_{dl} \cdot S)/C_s$, where S is the the geometric area of the working electrode and C_s is the specific capacitance of a smooth surface (generally assumed to be 0.04 mF cm^{-2} based on literatures).[1-4]

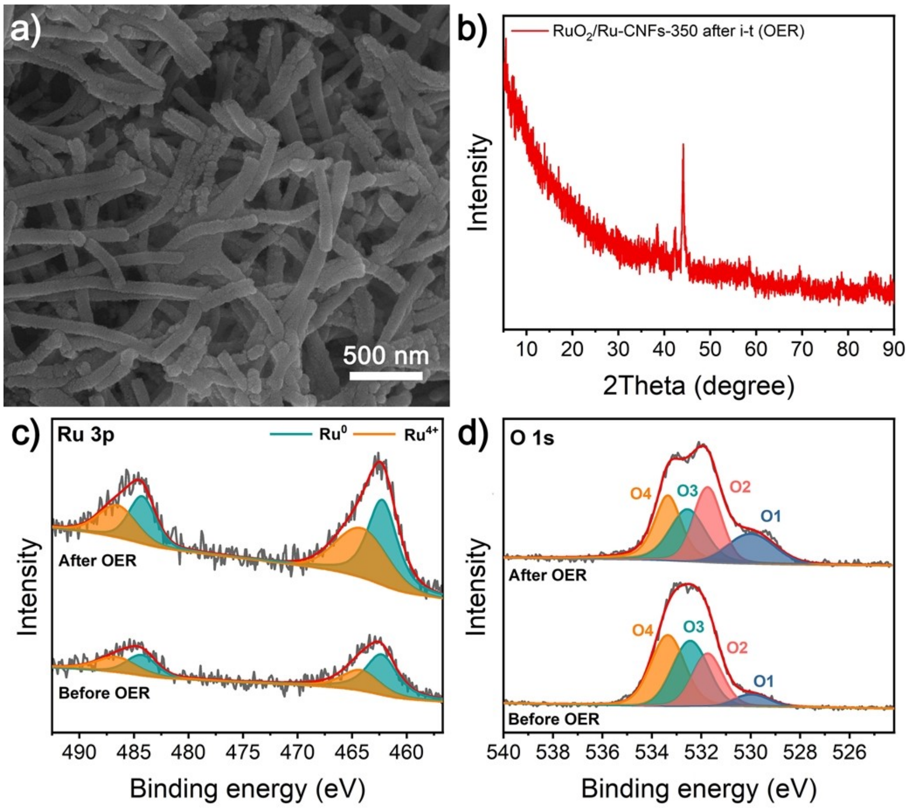

Fig. S15 (a) SEM image, (b) XRD pattern, and narrow-scan XPS spectra of (c) Ru 3p and (d) O 1s of RuO_2/Ru-CNFs-350 after the i-t measurement for OER.

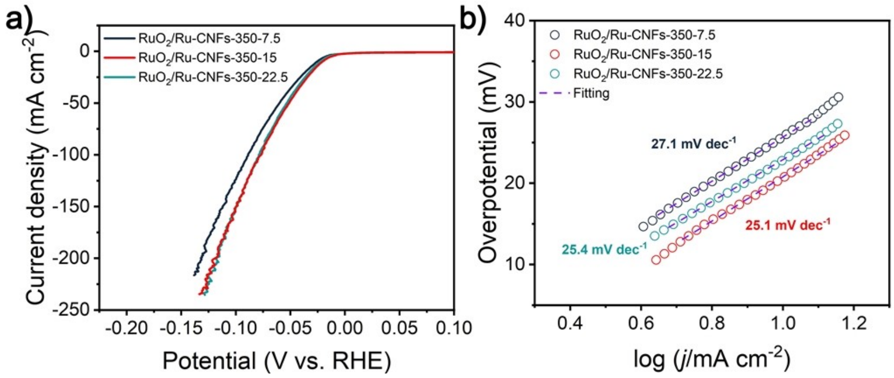

Fig. S16 (a) Polarization curves and (b) Tafel plots of different RuO_2/Ru-CNFs catalysts for HER in 1 M KOH.

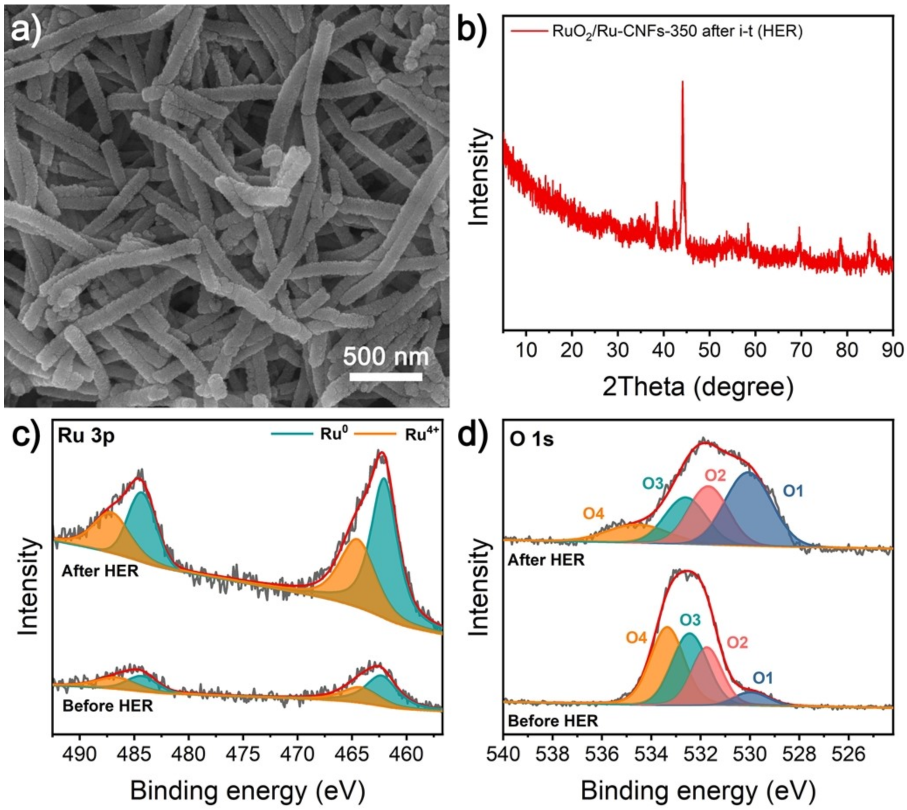

Fig. S17 (a) SEM image, (b) XRD pattern, and narrow-scan XPS spectra of (c) Ru 3p and (d) O 1s of RuO_2/Ru-CNFs-350 after the i-t measurement for HER.

Table S1 Comparison of some representative catalysts for OER properties in 1 M KOH.

Sample	Substrate	*j* (mA cm^{-2})	η (mV)	Tafel slope (mV dec^{-1})	Reference
RuO_2/Ru-CNFs-350	GCRDE[a)]	10	203	40.0	This work
		100	256		
		200	280		
Commercial RuO_2	GCRDE	10	339	91.5	This work
Ru-CoV-LDH/NF	NF[b)]	10	230	81.2	*ChemSusChem* 2021, **14**, 730.
RuO_2@$Zn_3V_3O_8$	CP[c)]	10	228	46	*ACS Appl. Mater. Interfaces* 2021, **13**, 54951.
$RuTe_2$-400	GCE[d)]	10	275	53	*Appl. Catal. B-Environ.* 2020, **278**, 119281.
Ru-NiCoP/NF	NF	20	216	84.5	*Appl. Catal. B-Environ.* 2020, **279**, 119396.
		100	285		
RuO_2/F-graphene	GCE	10	239	56	*Inorg. Chem. Front.* 2020, **7**, 2188.
CoNiFe LDH/$RuO_{2.1}$	GCE	10	281	48.9	*ACS Appl. Mater. Interfaces* 2020, **12**, 33083.
NiTe@RuO_2	NF	10	274	65	*Appl. Catal. B-Environ.* 2020, **272**, 118988.
Ru–MnFe/NF	NF	20	262	75	*Adv. Energy Mater.* 2020, **10**, 2000814.
Ru-RuO_2/CNT	GCE	10	210	64	*Nano Energy* 2019, **61**, 576.
0.27-RuO_2@C	GCRRDE[e)]	10	250	68	*Nano Energy* 2019, **55**, 49.
RuCu NSs	GCE	10	234	41.2	*Angew. Chem. Int. Ed.* 2019, **58**, 13983.
RuO_2/NiO/NF	NF	10	250	50.5	*Small* 2018, **14**, 1704073.
Ru NWs	GCE	10	224	46	*Adv. Funct. Mater.* 2018, **28**, 1803722.
Ru-RuP_x-Co_xP	GCE	10	291	85.4	*Nano Energy* 2018, **53**, 270.
Ru/Cu-doped RuO_2	GCE	10	204	56	*Small* 2018, **41**, 1803009.
Cu–RuO_2	GCE	10	240	NA	*Adv. Mater.* 2018, **30**, 1801351.

[a)] Rotating disk electrode made of glassy carbon; [b)] Ni foam; [c)] Carbon paper; [d)] Glassy carbon electrode; [e)] Rotating ring disk electrode made of glassy carbon.

Table S2 The fitting data of the EIS measurements of the RuO_2/Ru-CNFs-350 catalyst with other prepared control samples for OER.

Sample	R_{Ω} (Ω)	R_{ct} (Ω)
Ru-CNFs-15	5.99	695.2
RuO_2/Ru-CNFs-300	4.79	1431
RuO_2/Ru-CNFs-350	4.80	6.37
RuO_2/Ru-CNFs-400	4.82	6.79
RuO_2/Ru-CNFs-450	4.63	29.05

Table S3 Comparison of the ECSA values of the RuO_2/Ru-CNFs-350 catalyst with other prepared control samples.

Sample	C_{dl} (mF cm^{-2})	ECSA (cm^{-2})	RF[a)]
Ru-CNFs-15	16.17	79.23	404.25
RuO_2/Ru-CNFs-300	28.3	138.67	707.5
RuO_2/Ru-CNFs-350	140.6	688.94	3515
RuO_2/Ru-CNFs-400	118.9	582.61	2972.5
RuO_2/Ru-CNFs-450	30.7	150.43	767.5

[a)] RF is the roughness factor calculated by taking the estimated ECSA and dividing by the geometric area of the electrode, 0.196 cm^2.[4]

Table S4 Comparison of some representative catalysts for HER properties in 1 M KOH.

Sample	**Substrate**	***j* (mA cm^{-2})**	***η* (mV)**	**Tafel slope (mV dec^{-1})**	**Reference**
RuO_2/Ru-CNFs-350	GCRDE[a)]	10	21	25.1	This work
		50	51		
		150	99		
Commercial Pt/C	GCRDE	10	24	25	This work
Ru-CoV-LDH/NF	NF[b)]	10	32	36.4	*ChemSusChem* 2021, **14**, 730.
Ru/Co_4N-CoF_2	NF	10	53	144.1	*Chem. Eng. J.* 2021, **414**, 128865.
		100	199		
$RuTe_2$-400	GCE[c)]	10	34	28	*Appl. Catal. B: Environ.* 2020, **278**, 119281.
Ni_5P_4-Ru	GCE	10	123	56.7	*Adv. Mater.* 2020,1906972.
	CC[d)]		54	52	
(Ru–Co)O_x/CC	CC	10	44.1	23.5	*Angew. Chem. Int. Ed.* 2020, **59**, 17219.
RuO_2/F-graphene	GCE	10	49	31	*Inorg. Chem. Front.* 2020, **7**, 2188.
SA-Ru-MoS_2	GCE	10	76	21	*Small Methods* 2019, **3**, 1900653.
Ru/Ni$(OH)_2$/NF	NF	10	25	47	*J. Mater. Chem. A* 2019, **7**, 11062.
RuB_2	GCE	10	28	28.7	*Adv. Energy Mater.* 2019, **9**, 1803369.
Sr_2RuO_4	GCRDE	10	61	51	*Nat. Commun.* 2019, **10**, 149.
Ru ND/C	GCE	10	43.4	49	*Chem. Commun.* 2018, **54**, 4613.
RuO_2/NiO/NF	NF	10	22	31.7	*Small* 2018, **14**, 1704073.
Ru@GnP	RRDE[e)]	10	22	28	*Adv. Mater.* 2018, **30**, 1803676.
Ru NP/C	GCE	50	69	33	*Adv. Energy. Mater.* 2018, **8**,1801698.
RuCoP	GCE	10	23	37	*Energ. Environ. Sci.* 2018, **11**, 1819.
Ru_2P nanoparticles	GCE	10	54	29.3	*Nat. Nanotechnol.* 2017, **12**, 441.
RuP_2@NPC	GCE	10	52	69	*Angew. Chem., Int. Ed.* 2017, **56**, 11559.

[a)] Rotating disk electrode made of glassy carbon; [b)] Ni foam; [c)] Glassy carbon electrode; [d)] Carbon cloth; [e)] Rotating ring disk electrode made of glassy carbon.

Table S5 The fitting data of the EIS measurements of the RuO_2/Ru-CNFs-350 catalyst with other prepared control samples for HER.

Sample	**R_{Ω}(Ω)**	**R_{ct} (Ω)**
Ru-CNFs-15	5.07	5.49
RuO_2/Ru-CNFs-300	5.14	13.60
RuO_2/Ru-CNFs-350	5.16	3.26
RuO_2/Ru-CNFs-400	4.88	8.48
RuO_2/Ru-CNFs-450	4.94	14.09

Table S6 Comparison of some representative catalysts for overall water splitting properties in 1 M KOH.

Electrolyzer (Cathode||Anode)	Substrate	Voltage@10 mA cm^{-2} (V)	Reference
RuO_2/Ru-CNFs-350|| RuO_2/Ru-CNFs-350	Ni foam	1.452	This work
Commercial Pt/C|| Commercial RuO_2	Ni foam	1.560	This work
Ru-CoV-LDH/NF|| Ru-CoV-LDH/NF	Ni foam	1.5	*ChemSusChem* 2021, **14**, 730.
(Ru-Co)O_x/CC|| (Ru-Co)O_x/CC	Carbon cloth	1.488	*Angew. Chem. Int. Ed.* 2020, **59**, 17219.
$RuTe_2$-400||$RuTe_2$-400	Glassy carbon electrode	1.57	*Appl. Catal. B-Environ.* 2020, **278**, 119281.
Ru-NiFe-P||Ru-NiFe-P	Ni foam	1.47	*Appl. Catal. B: Environ.* 2020, **263**, 118324.
Ru-MnFeP/NF|| Ru-MnFeP/NF	Ni foam	1.47	*Adv. Energy Mater.* 2020, 2000814
Ru-NiCoP/NF|| Ru-NiCoP/NF	Ni foam	1.515	*Appl. Catal. B-Environ.* 2020, **279**, 119396.
RuO_2/F-graphene|| RuO_2/F-graphene	Glassy carbon electrode	1.56	*Inorg. Chem. Front.* 2020, **7**, 2188.
NiTe@RuO_2|| NiTe@NiFe-LDH	Ni foam	1.49	*Appl. Catal. B-Environ.* 2020, **272**, 118988.
RuIrO_x||RuIrO_x	Carbon fiber paper	1.47	*Nat. Commun.* 2019, **10**, 4875.
0.27-RuO_2@C|| 0.27-RuO_2@C	Rotating ring disk electrode	1.50	*Nano Energy* 2019, **55**, 49.
RuCu NSs/C-250 °C|| RuCu NSs/C-350 °C	Glassy carbon electrode	1.49	*Angew. Chem. Int. Ed.* 2019, **58**, 13983.
Ru/Cu-doped RuO_2|| Ru/Cu-doped RuO_2	Glassy carbon electrode	1.47	*Small* 2018, **14**, 1803009.
Ir NWs||RuO_2 NWs	Glassy carbon electrode	1.47	*Adv. Funct. Mater.* 2018, 1803722
RuO_2/NiO/NF|| RuO_2/NiO/NF	Ni foam	1.5	*Small* 2018, 1704073
NiFeRu-LDH/NF|| NiFeRu-LDH/NF	Ni foam	1.52	*Adv. Mater.* 2018, 30.

References

1 S. Chen, H. Huang, P. Jiang, K. Yang, J. Diao, S. Gong, S. Liu, M. Huang, H. Wang and Q. Chen, Mn-doped RuO_2 nanocrystals as highly active electrocatalysts for enhanced oxygen evolution in acidic media, *ACS Catal.*, 2019, **10**, 1152.

2 J. D. Benck, Z. Chen, L. Y. Kuritzky, A. J. Forman and T. F. Jaramillo, Amorphous molybdenum sulfide catalysts for electrochemical hydrogen production: Insights into the origin of their catalytic activity, *ACS Catal*., 2012, **2**, 1916.

3 B. Chen, X. He, F. Yin, H. Wang, D. J. Liu, R. Shi, J. Chen and H. Yin, MO-Co@N-doped carbon (M = Zn or Co): Vital roles of inactive Zn and highly efficient activity toward oxygen reduction/evolution reactions for rechargeable Zn–air battery, *Adv. Funct. Mater.*, 2017, **27**, 1700795.

4 C. C. McCrory, S. Jung, J. C. Peters and T. F. Jaramillo, Benchmarking heterogeneous electrocatalysts for the oxygen evolution reaction, *J. Am. Chem. Soc.*, 2013, **135**, 16977.